Static and Dynamic Behavior of H_2O and O_2 Penetrants in a Polybenzoxazine

Won-Kook Kim and Wayne L. Mattice*

Maurice Morton Institue of Polymer Science, The University of Akron, Akron, Ohio 44325-3909

Received April 27, 1998; Revised Manuscript Received October 23, 1998

ABSTRACT: The diffusion of water and oxygen molecules in the polybenzoxazine (PBO) matrix was studied at 295 and 450 K using fully atomistic molecular modeling. The hydrogen bonding of water and the hydroxyl groups in PBO is evident in the pair correlation function. The predicted diffusion coefficients for the two penetrants are remarkably close, although water forms hydrogen bonds with PBO but oxygen does not. The averaged hydrogen bond fraction and hydrogen bond lifetime were studied using the hydrogen-bonding autocorrelation function. The lifetime of the hydrogen bond between water and PBO is much shorter than the average residence time of the penetrant in a cavity, and therefore, the hydrogen bond does not remarkably retard the diffusion of water in the PBO matrix. The association of water is also observed.

Introduction

The investigation of the diffusion of small penetrants through a polymer matrix has a long history,[1−3] since this physical process is very important in technologies such as packaging, pervaporation, separation, and drug implants. To understand the mechanism of the penetrant diffusion in the polymer matrix, consideration at the molecular or atomistic level is essential. The elastic response of the matrix upon the collision of the penetrants, local mobility of the polymer matrix, free volume shape and size distribution, and the interaction between diffusants and polymer matrix all contribute to the diffusion of small molecules in a polymer matrix.[4] Owing to these complexities, there remain unanswered questions about the diffusion process in a polymer matrix.

The diffusion of small particles in a polymer matrix has been described as similar to a random walk process on a long time scale. Molecular dynamics (MD) simulation is useful to attain an understanding of molecular level fundamentals and the diffusion coefficient of small penetrants. From the trajectories, not only the diffusion coefficient but also the diffusion mechanism on a microscopic scale can be obtained. With the recent computer capabilities, time scales up to nanoseconds of fully atomistic simulation are accessible, and on this time scale, the diffusion path of very small penetrants is sometimes random. An alternative method to predict the diffusion coefficient, the transition-state approach,[5] is coarse-grained on the basis of the assumptions: (i) the movement of small molecules is composed of a series of activated hops; (ii) the structural relaxation of the polymer matrix does not affect the penetrant dynamics. This technique might be useful for slower diffusion processes, which are not accessible by fully atomistic MD simulation.

In the 1990s, many MD simulation studies of diffusion in amorphous polymers have been reported[6−22] aiming at either direct prediction of diffusivities or the elucidation of fundamental aspects of penetrant motion in a polymer matrix. Most studies use a structurally simple polymer matrix, such as polyethylene,[7,9,16,19] polypropylene,[12] polyisobutylene,[16] or poly(dimethylsiloxane),[13,18] with a few studies of more complex polymers such as polystyrene,[22] polycarbonate,[12,21] and the amorphous portion of a semicrystalline polyimide.[20] Many of the early MD studies[7−11] failed to obtain the experimentally determined diffusion coefficient, which may result from coarse graining of the polymer structure by employing a united atomic force field. Much improved results are obtained by introducing explicit hydrogen atoms into the model of polyisobutylene.[14] However, the qualitative description of diffusion from MD simulation can successfully reproduce experimental observations[23−26] such as the effect of the diffusant size,[6] temperature and density on the diffusion coefficients,[6,10] and anomalous diffusion at short times.[15,17]

In this work, the diffusion of O_2 and H_2O in bulk polybenzoxazine (PBO) at two different temperatures, i.e., below T_g and near or above T_g, was studied using fully atomistic MD simulation. PBO can form hydrogen bonds with water molecules, and O_2 is larger than H_2O. Therefore, the competition between the steric effect and the hydrogen bonding can be expected in the diffusion of water and oxygen molecules. The temperature effect on the hydrogen bonding can also be studied. Another motivation to study the diffusion in PBO is that this material has an exceptional flame retardency. Similar work[14] can be found in the coarse-grained MD technique, which focused on the effect of the size and the attraction between polymer and diffusants by employing a series of different σ and ϵ in the van der Waals interaction.

Methods

The simulation was performed with the software package Discover from Molecular Simulations, Inc. and the PCFF force field.[27−29] The bulk amorphous PBO structures were constructed from a single unperturbed chain packed into a cubic periodic cell at the desired density followed by relaxation above T_g and then minimization of the energy.[30] Bond stretching was suppressed in the current work, but all of the other energy terms used previously[30] were included. Since the size of the diffusant is relatively large (radius of O is 1.5 Å), the effect of bond stretching of the polymer matrix may be less important for the hopping of the diffusants than the bending and torsion of the side groups such as the O−C bond or methyl side group in PBO matrix. The reliability of the charges assigned in the PCFF force field is discussed in the recent study of the

10.1021/ma9806662 CCC: $15.00
Published on Web 12/09/1998

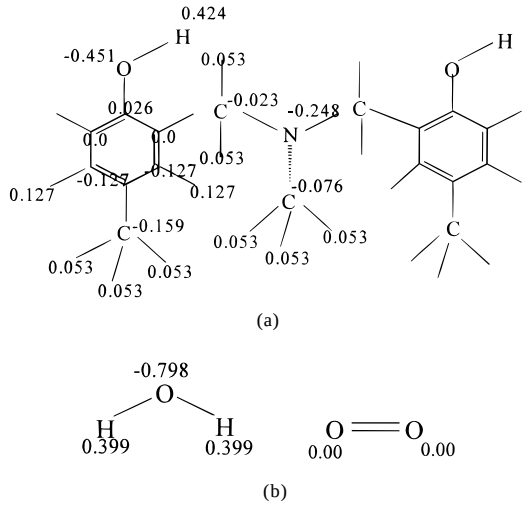

Figure 1. Assigned charge for (a) PBO and (b) penetrants water and oxygen.

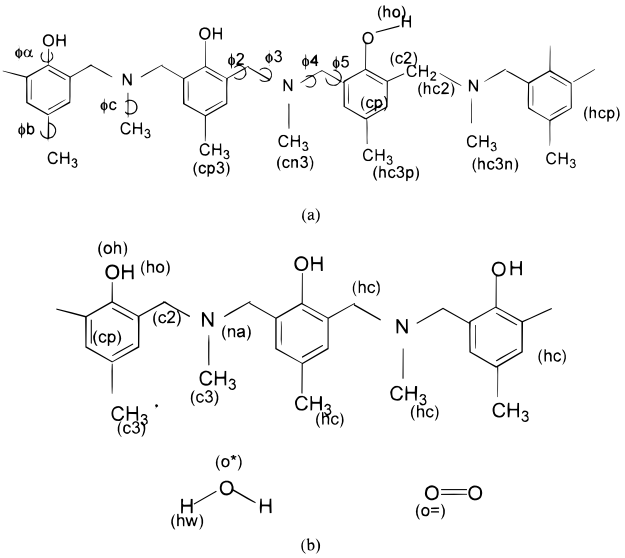

Figure 2. Definition (a) of seven torsion angles in PBO as well as atom types and (b) PCFF potential type assignments of atoms.

diffusion of water−ethanol mixtures in poly(dimethylsiloxane).[31] All partial charges q_i of the atoms of the PBO and the diffusants are shown in Figure 1. The Coulombic energy was calculated according to

$$\sum_{i>j} \frac{q_i q_j}{\epsilon r_{ij}} \tag{1}$$

where ϵ is the dielectric constant and r_{ij} is the distance between two particles i and j. In this study, the dielectric constant is treated as unity. The notations of the assigned potential types for all atoms and the torsion angle assignments as well as the atom type assignments are shown in Figure 2. The main differences in the types of O in water and in the polymer are charge and bending energy, but the van der Waals parameters are very close to each other. The potential type of oxygen in diatomic oxygen molecule is assigned as o= for an oxygen atom with double bonds. The van der Waals energy parameters are listed in Table 1 for the atoms in PBO, water, and O_2.

To reduce the structure dependence of the diffusion, two or three bulk PBO structures were employed as the media for the simulation. The centers of the clustered voids detected by introducing a hard sphere probe with a radius of 1 Å into the system were determined for these structures.[30] Three or four

Table 1. van der Waals Energy[a] Parameters Employed for Simulation

	r_0 (Å)	ϵ (kcal/mol)
oh (PBO)	3.535	0.24
na (PBO)	4.07	0.065
cp (PBO)	4.01	0.064
c2 (PBO)	4.01	0.054
c3 (PBO)	4.01	0.054
ho (PBO)	1.098	0.013
hc (PBO)	2.995	0.02
o= (O_{2O})	3.535	0.06
o* (H_{2O})	3.608	0.274
hw (H_{2O})	1.098	0.013

[a] $E = \epsilon_{ij}[2(r_{ij}^*/r_{0,ij})^9 - 3(r_{ij}^*/r_{0,ij})^6]$ where $r_{0,ij} = [(r_{0,i}^6 + r_{0,j}^6)/2]^{1/6}$ and $\epsilon_{ij} = 2[(\epsilon_i + \epsilon_j)]^{1/2} r_{0,i}^3 r_{0,j}^3/(r_{0,i}^6 + r_{0,j}^6)$.

voids were found with volume greater than 1 Å^3, and the mass center of the diffusants was located with arbitrary orientations in these positions so that the diffusants can be inserted without severe steric repulsion from well-relaxed bulk PBO at the start of the simulation. The cubic periodic boundary conditions were applied with the periodicities of 20.075 and 20.723 Å for 295 and 450 K, respectively. The densities are 1.10 g/cm^3 at 295 K, which is comparable to the experimental density of the PBO resin[32] (1.12 g/cm^3), and 1.0 g/cm^3 at 450 K. The equilibrium content of water in PBO was measured[32] at room temperature as 1.3%, which corresponds to three to four water molecules in each cell. Similar amounts of water molecules were implanted in these cells at 450 K. The dependence of the diffusion on the concentration of penetrants is negligible in this dilute concentration regime. The energy of the system was minimized before the MD run to relax the local bad contacts.

The MD trajectories were sampled under *NVT* conditions with the velocity Verlet algorithm, and the temperature was controlled by direct velocity scaling whenever the temperature deviated more than 20 K from the target. The SHAKE algorithm was used to achieve a relatively long trajectory within feasible computational time. Consequently, a time step of 3 fs can be used without overstretching of the covalent bonds.

For the diffusion of water, the sampling of the coordinates of atoms and velocities was started after 400 ps and was carried out every 1 ps up to 1.5 ns. For the diffusion of diatomic oxygen molecules, the length of the trajectory is 600 ps using the same procedure, and the sampling starts after 50 ps. Eleven diffusants were introduced in three independent structures at 295 K, while seven diffusants were introduced in two independent structures at 450 K.

Results and Discussion

1. Estimation of the Diffusion Coefficients of H_2O and O_2 in PBO. The underlying process of the penetrant diffusion is a hopping mechanism. The penetrants reside in voids that are present in amorphous polymers for a considerable time period, with only a small amplitude of oscillating movement. Occasionally, a rapid hop into a neighboring void occurs. Several hops of the water molecules in a PBO matrix can be observed in Figure 3. Trajectories were obtained from the center of mass of four water molecules in PBO at 450 K. To monitor relatively large movement, consecutive points are shown every 10 ps. If the periodic boundary conditions are applied in the display, one can notice that some locations of the amorphous cells are never visited by the diffusant molecules, while some other locations are frequently visited by more than one diffusant. As stated in an earlier study,[20] this may indicate that (i) certain paths and locations, which can correspond to the free-volume voids, are favored by all diffusants and (ii) there is no substantial structural relaxation of the polymer during the simulation, which agrees with the assump-

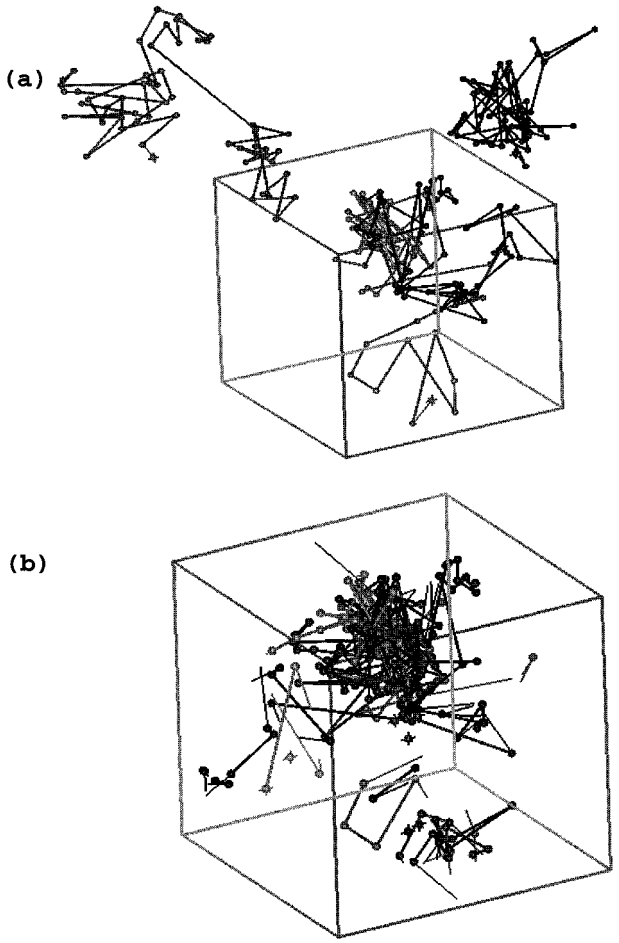

Figure 3. Trajectories of the center of mass of four water molecules in PBO at 450 K. The time between consecutive points is 10 ps. Part b is identical with part a except for the compression of the coordinate into the unit cell. The polymer matrix is not shown in the figure.

tions of Gusev et al.[17] Trajectories obtained at 295 K (not shown) reveal very few hops of either H_2O or O_2, which implies that the rare hopping of the water molecule at 295 K does not result from the hydrogen bonding between water and PBO but results instead from the almost frozen PBO matrix.

The local dynamics of the PBO matrix at these temperatures were studied with a torsional autocorrelation function (TACF), which can be described as

$$G(t) = \langle \cos[\phi(t) - \phi(0)] \rangle \tag{2}$$

where the angle brackets represent averaging over all the time origins. Figure 4 shows the TACFs for seven independent bonds in PBO at two different temperatures. At 295 K, the TACFs (except the two for bonds to methyl groups) show plateaus caused by the suppression of conformational transitions from one potential well to another, with only oscillations within a single potential well. Conformational transitions are available at 295 K within several picoseconds for ϕb and ϕc, which are torsional angles of $C-CH_3$ and $N-CH_3$, respectively. These bonds are relatively easy to rotate, compared to the backbone bonds, as is also true for the C−O bonds. At room temperature, the TACF of the C−O bond shows a plateau around 0.67, which is roughly equivalent to the value of $\cos(\pi/6)$. The hydrogen-bonding constraints on the C−O bond may prevent rotation as easily as for ϕb and ϕc and produce the plateau around 0.67. At 450

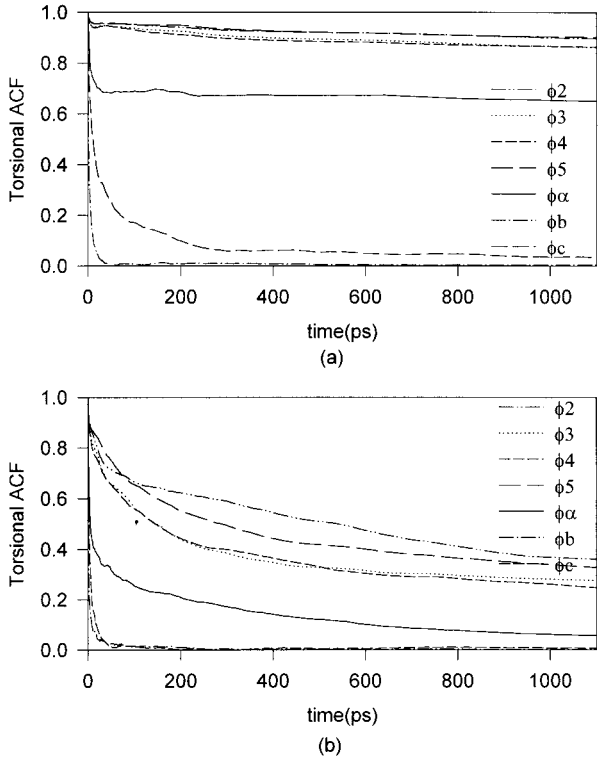

Figure 4. Torsional autocorrelation function for bonds in PBO in the presence of water molecules at (a) 295 K and (b) 450 K. Angles are identified in Figure 2.

K, the rotational transition of the backbone bonds is apparent in the decay of the TACF. The diffusants can move around within the PBO matrix as a result, and hopping of the diffusants into the neighboring voids can be expected within feasible time periods.

The diffusion coefficient can be calculated from the mean square displacement of the centers of mass of all n diffusants averaged over time as

$$D = \frac{1}{6t}\left\langle \sum_{i=1}^{n} r_i^2 \right\rangle \tag{3}$$

where n is equal to 11 and 7 for 295 and 450 K, respectively. The mean square displacement of each diffusant differs within an order of magnitude as a function of time interval because of the unique local environment surrounding each diffusant. To obtain a more accurate estimate of the diffusion coefficient, better statistics may be required, such as longer trajectories and more PBO structures and diffusants, etc. But the current sampling size is enough to achieve an estimate of the diffusion coefficient of water and oxygen and to study the effect of the hydrogen bonding on the diffusion mechanism. The averaged mean square displacements of the centers of mass of water and O_2 are shown in Figure 5. It is known from the earlier studies that the hopping mechanism is the underlying process of the diffusion. However, in the trajectories at 295 K, the hopping of the diffusant molecules is rarely observed for both systems. Much longer trajectories would be essential to get enough sampling of the hopping of the diffusants. The estimated diffusion coefficients of H_2O and O_2 at 450 K are 6.8×10^{-10} and 6.5×10^{-10} m^2/s, respectively. The strikingly small difference in the diffusion coefficients of the two diffusants in PBO at 450

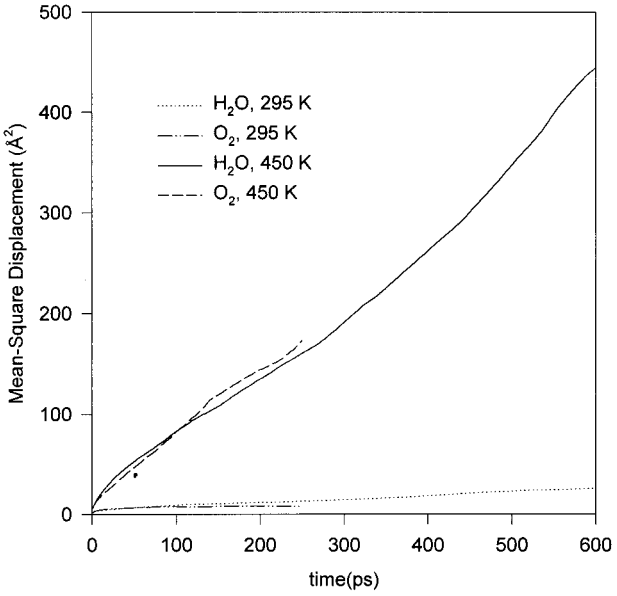

Figure 5. Averaged mean square displacement of the diffusant molecules as a function of time interval in PBO at 295 and 450 K. The trajectories for O_2 are shorter than those for H_2O.

K is interesting in view of their different abilities to form hydrogen bonds with the matrix.

2. Comparison of the Local Environments around Water and Oxygen Molecules. Since PBO has a strong partial charge assigned to some of its atoms, the interatomic interactions between a specific pair of atoms in polar diffusants and the polymer matrix may exhibit preferences over the rest of the atom pairs. Therefore, the pair correlation functions between specific pairs of atom types were studied. The pair distribution functions for the different types of atoms in PBO with the H_2O at 295 K are depicted in Figure 6. Similar results (not shown) are obtained at 450 K. The hydrogen bonding between water and PBO can be inferred from the very intense sharp peak around the arrows for the two $g(r)$ that involve the hydroxyl group in the phenol. For the rest of the atom pairs, peaks appear at a greater distance than the sum of hard sphere radii, indicating that repulsion is dominant. Even at the elevated temperature, the attractive interaction between water and the hydroxyl group in PBO is present, on the basis of the pair correlation functions. No remarkable changes of $g(r)$, especially at relatively short separation, were observed for the two temperatures. For three different types of carbon atoms, the C3 atom is the most accessible to the water molecules on the basis of the largest peak area and its position in the pair correlation function.

The pair distribution functions of oxygen (O═) in the diatomic oxygen molecule and atoms in PBO are shown in Figure 7 (at 295 K). Similar results (not shown) are obtained at 450 K. Sharp intense peaks are not seen in the pair correlation functions of the O═ and H(O) pair and the O═ and O(H) pair near the sum of hard sphere radii for water and PBO system. This result is in marked contrast to the behavior seen when water is present. Amid all types of carbon atoms, the C3 atom is the most exposed to the oxygen molecule, considering the peak area and position in the pair correlation functions.

The intermolecular pair correlation functions between oxygen atoms in the diffusants are shown in Figure 8.

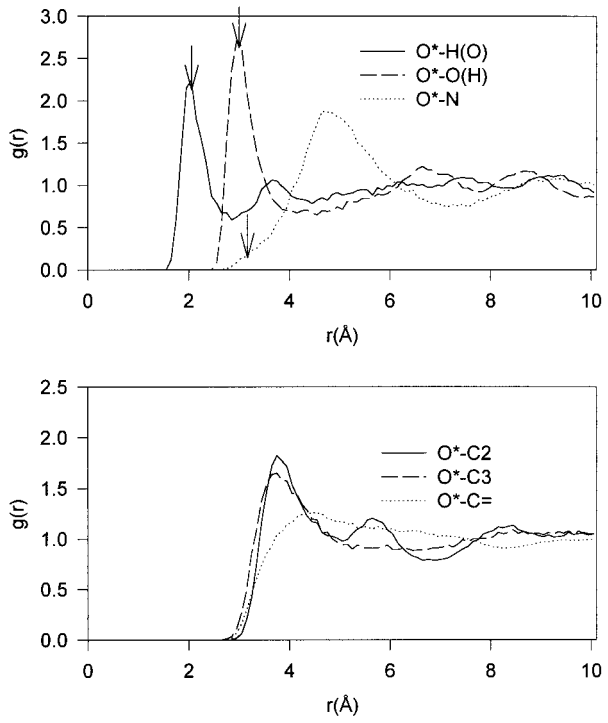

Figure 6. Radial distribution function of the oxygen atom of water with selected atoms in the PBO matrix at 295 K. The arrows on the curves indicate the sum of the hard sphere radii of the atoms.

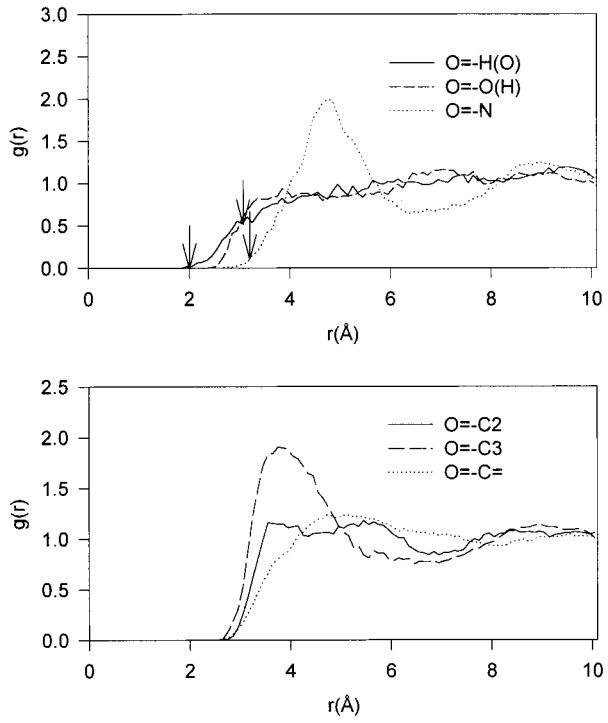

Figure 7. Radial distribution functions of the oxygen atom in an O_2 molecule with selected atoms in the PBO matrix at 295 K. The arrows on the curves indicate the sum of the hard sphere radii of the atoms.

The sharp intense peaks located near 2.6 Å provide evidence of the self-aggregation of water molecules. Considering the larger peak area at 450 K than that at 295 K, the water molecule can form aggregates more easily at elevated temperature because of two contributions such as (i) increased chance of a void within the PBO matrix, which is big enough to hold more than one

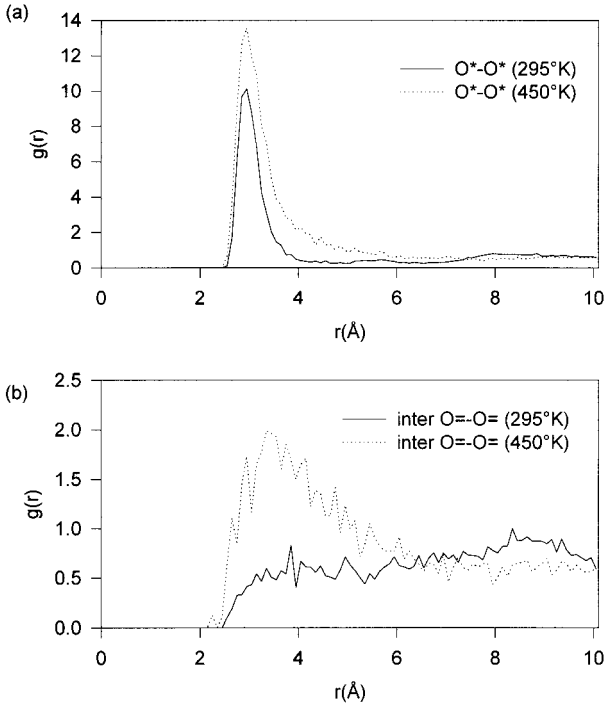

Figure 8. Intermolecular radial distribution function of (a) O−O of water molecules and (b) O−O of diatomic oxygen molecules at 295 and 450 K.

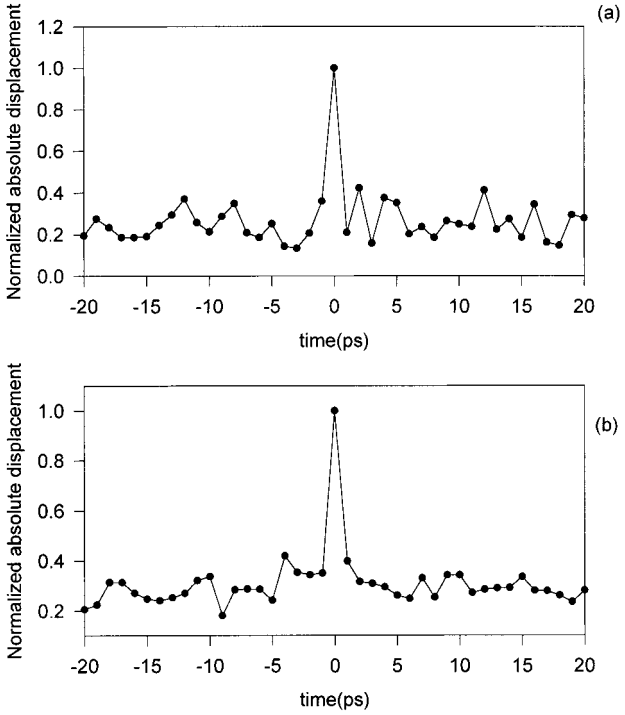

Figure 9. Normalized absolute displacement of water molecules in PBO matrix at 295 K (a) and 450 K (b). $t = 0$ ps is the time frame when the absolute displacement of water is greater than 7 Å.

penetrant, and (ii) increased kinetic energy, which can provide more chance for binary encounters during the simulations. The diffuse peak in $g(r)_{O=O=}$ in diatomic oxygen molecule might result from the above contributions as well. However, once the water molecules can get close enough to form hydrogen bonding, they can easily form aggregates, while the oxygen molecules cannot form stable aggregates, since there is no strong attractive force between them.

The local environments around the diffusant water and diatomic oxygen molecule are markedly different from each other because of the differences in the pair correlation functions. The sharp peaks in water and hydroxyl group in the PBO pair correlation function provide strong evidence of hydrogen bonding between them, although the pair correlation function alone does not afford any information about the O···HO angle.

3. Detailed Analysis of the Diffusion of Water in PBO. 3.1. Hopping Process. The hopping event of a small penetrant from a cavity to a neighboring cavity is the underlying process of its diffusion in a polymer matrix, since this process can occur in a fairly short time period with a large amount of displacement, compared to the pseudostationary time period of the penetrant in a cavity with a long residence time with trivial displacements. There are two interesting questions about this process. (i) What is the time scale of the hopping process? (ii) Which part of the molecular motion can be related to the opening of the channel in a hopping event? To answer these questions, the absolute displacement of the penetrants at every picosecond was obtained. When the absolute displacement is greater than 7 Å, then a jump event was assumed at the corresponding time frame, and the previous 20 ps of absolute displacements and the next 20 ps of absolute displacements were recorded and accumulated for the whole jump events. Twenty six events were found from seven penetrants in two independent PBO structures at 450 K, while four jump events were found from 11 penetrants in three independent PBO structures at 295 K. The accumulated absolute displacements were then normalized with that of the displacement at the jump event. In Figure 9, the normalized absolute displacements around the jump event are shown for two temperatures. Regardless of the temperature, the normalized displacements very near the jump event are not considerably different from those of the previous 20 ps and the next 20 ps of jump event, implying that the opening of a channel in the polymer matrix, which provides the path to jump to a neighboring cavity for the penetrants, occurred on a very short time scale.

The absolute displacement of the atoms in the polymer at every jump event was calculated as functions of their locations from the penetrant and is shown in Figure 13. Region I is assigned for the atoms located within 5 Å of the center of the water molecule at the jump event, and for the rest of the atoms, region II is assigned. At 295 K, among atoms in region I, only methyl groups attached to the phenyl ring positioned para to the hydroxyl have a higher absolute displacement than those in region II. All types of atoms in region I have higher absolute displacements than those in region II at 450 K. At 295 K, the penetrant might prefer a special path to jump into the neighboring cavity, using a channel that is opened by the displacement of the methyl group attached to the phenyl ring. From the torsional autocorrelation function, the only available torsional transitions were found to be in the side groups at this temperature. In contrast, at 450 K, the water molecule can jump into a neighboring void via several paths, since at this temperature, the torsional transition of the backbone bonds is available as well.

3.2. Averaged Number of Hydrogen Bonds in the System. The hydrogen bonds can be defined from the separation distances and angles between donors and

Table 2. Average Number of Hydrogen Bonds at Two Temperatures When the Donor Is the Hydroxyl Group in (a) PBO and in (b) Water

(a)

	295 K (65% HO)	450 K (52.4% HO)
OH (33)	6.26 (29.3% of acceptor)	3.3 (19.1% of acceptor)
N (32)	14.3 (66.8% of acceptor)	13.2 (76.3% of acceptro)
WO (3.67, 3.5)[a]	0.83 (3.93% of acceptor)	0.8 (4.6% of acceptor)

(b)

	295 K (37.6% WH)	450 K (38.5% WH)
OH (33)	0.82 (59.4% of acceptor)	0.79 (58.6% of acceptor)
N (32)	0.06 (4.4% of acceptor)	0.06 (4.4% of acceptor)
WO (3.67, 3.5)[a]	0.5 (36.2% of acceptor)	0.5 (37% of acceptor)

[a] The numbers of water molecules are 11 and 7 for 295 and 450 K, respectively. The number inside the parentheses indicates the mean number of donors and/or acceptors for each cell.

acceptors. The pair correlation function does not give any information about the angle, but it can provide strong indication of hydrogen bonding based on the sharp peak positioned around the sum of the hard sphere radii between oxygen atom pairs in PBO and water. The hydrogen bonds were assumed in the present study whenever the distance between donor and acceptor is less than 2.5 Å and the absolute angle of H−O···O is greater than 120°. The donor includes (O)H in PBO and water, and the acceptor includes N, O(H) in PBO and O(H) in water molecules. The averaged number of hydrogen bonds can be calculated from the trajectories as

$$\langle n_{\mathrm{hb}} \rangle = \frac{\sum_{j=1}^{m}\sum_{i=1}^{l} n_{\mathrm{hb}}}{ml} \tag{4}$$

where m is equal to the number of structures and l is number of snapshots in each structure. The averaged numbers of hydrogen bonds are listed in Table 2. When the donor was provided by the hydroxy group in PBO, the normalized amount of hydrogen bonds at 295 K (about 65% of H(O) from PBO participated in hydrogen bonds) is relatively greater than those at 450 K (about 52.4% of H(O) from PBO participating in hydrogen bonds). The 65% of OH group participation in the hydrogen bonds at 295 K is very similar to the predicted fraction of hydrogen bonds in PBO bulk at 1.1 g/cm^3, which corresponds to the density at 295 K.[30] The introduction of water molecules into PBO does not strongly affect the total hydrogen bond fraction in the system. When the donor was provided by the hydroxyl group in the water molecule, the normalized hydrogen bond amounts at 450 K (38.5%) are comparable to those at 295 K (37.6%).

For the hydrogen bonds whose donors are provided from PBO, about $^2/_3$ of acceptors are the nitrogen atoms in PBO, which agrees with the prediction from the static bulk structures[30] and is consistent with the spectroscopic properties of model PBO oligomers.[33] For the hydrogen bonds whose donors are provided from water molecules, about 60% of acceptors are from the hydroxyl groups in PBO and also a considerable fraction of intermolecular hydrogen bonds between water molecules is seen. Hydrogen bonds between a water molecule and nitrogen atom in PBO are rarely found at both temperatures.

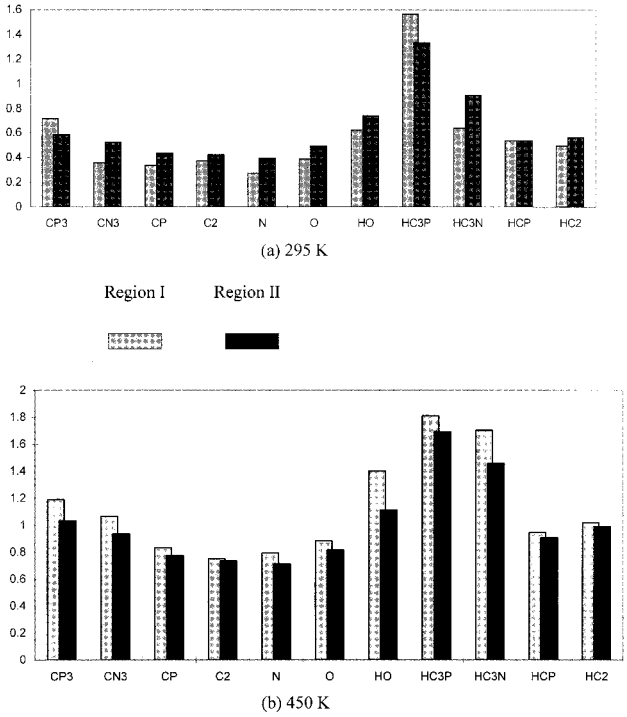

Figure 10. Normalized absolute displacements of various types of atoms in PBO. Region I is defined so that the interatomic distance between the diffusant that just experienced hopping and atoms are within 5 Å, while region II is the rest of the region within the simulation box.

3.3. Stability of the Hydrogen Bonds. One of the methods to investigate the stability of the hydrogen bonds is to study the correlation of the orientational relaxation of water molecules, which can be simply described as

$$P = \left\langle \sum_{t=0} \frac{\mu(0)\cdot\mu(t)}{|\mu(0)||\mu(t)|} \right\rangle \tag{5}$$

where μ is the vector from the center of mass to the oxygen atom in the water molecule. The water molecule can be easily liberated from its initial position if the hydrogen bonds are weak enough so that the orientational correlation function will decay rapidly. A rapid initial decay of the curves is shown at both temperatures in Figure 11. The water molecules can alter their orientations easily despite the considerable presence of hydrogen bonds as shown in Table 2.

An alternative method to study the stability of the hydrogen bonds can be carried out from the hydrogen bonding autocorrelation functions, which is designed as

$$H(t) = \frac{\langle \sum_j \sum_i h_i(t(\mathrm{hb}) + t_0(\mathrm{hb}))\cdot h_i(t_0(\mathrm{hb}))\rangle}{\langle \sum_j \sum_i h_i(t_0(\mathrm{hb}))\rangle} \tag{6}$$

where $h_i(t(\mathrm{hb}))$ is defined for an atom pair i as

$$h_i(t(\mathrm{hb})) = 1 \quad \text{(hydrogen bonds)}$$
$$= 0 \quad \text{(non-hydrogen bonds)}$$

and t is time. This time is reset to be zero whenever the hydrogen bond was observed. The total number of scans to assign the values for h_i for each atom pair i

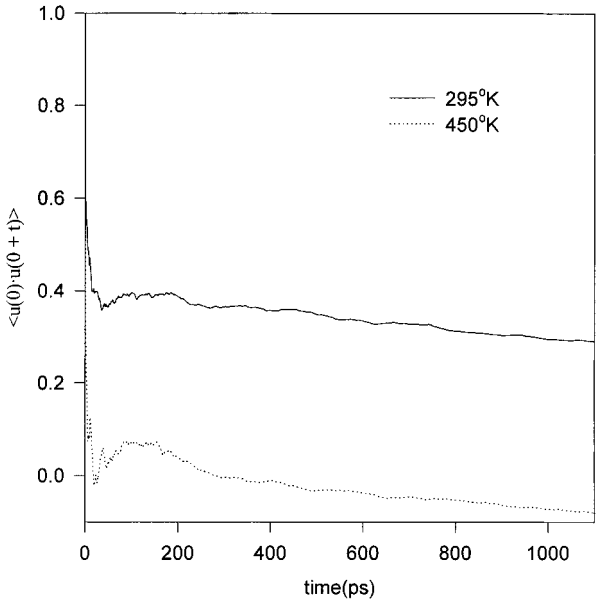

Figure 11. First-order orientational autocorrelation function of the vector from center of mass to the oxygen atom of a water molecule.

will be equivalent to the total number of hydrogen bonds between these atom pairs during $l - \tau$ ps, where l is equal to total simulation time and τ is equal to the scan interval. In this calculation, 1100 and 20 ps were employed as l and τ, respectively. If the hydrogen bonds between atom pairs i could stay for the scanning time interval τ, then $H(t)$ will be unity for every time period, while if the hydrogen bonds are too weak to be held even for 1 ps, then $H(t)$ will drop to zero except for t of 0 ps.

The lifetime of hydrogen bonds whose donor is provided from PBO is longer than that from water molecules for both temperatures, as shown by the $H(t)$ in Figures 12 and 13. There is a substantial decrease of $H(t)$ at 450 K from 295 K, suggesting that the increase of temperature shortens the lifetime of hydrogen bonds. The hydrogen bonds whose donors are provided by hydroxy groups in PBO have the longest lifetime with nitrogen atoms as acceptors, and they have the shortest lifetime with oxygen atom from water molecules as acceptors. At 295 K, the hydrogen bonds whose donors are provided by hydroxy groups in water have the longest lifetime with oxygen atom from PBO as acceptors and have the shortest lifetime with nitrogen atom from PBO as acceptors.

The conclusion that can be drawn from such a hydrogen bond correlation function of water molecules at 450 K is that the hydrogen bond lifetime of the water molecule is fairly short; i.e., the hydrogen bonds do not retard considerably the diffusion of water in the PBO matrix. Therefore, the diffusion of the water molecule is not strikingly lower than the diffusion of the oxygen molecule but is comparable to that of the oxygen molecule.

Summary

The diffusion coefficient of H_2O is very close to that of O_2 at 450 K, although the H_2O forms hydrogen bonds with PBO, but O_2 does not form hydrogen bonds. Much longer dynamics is essential to attain reliable diffusion coefficients at 295 K, since the jump event of the diffusant in the PBO matrix, which is the underlying process of the diffusion, can hardly be observed at this

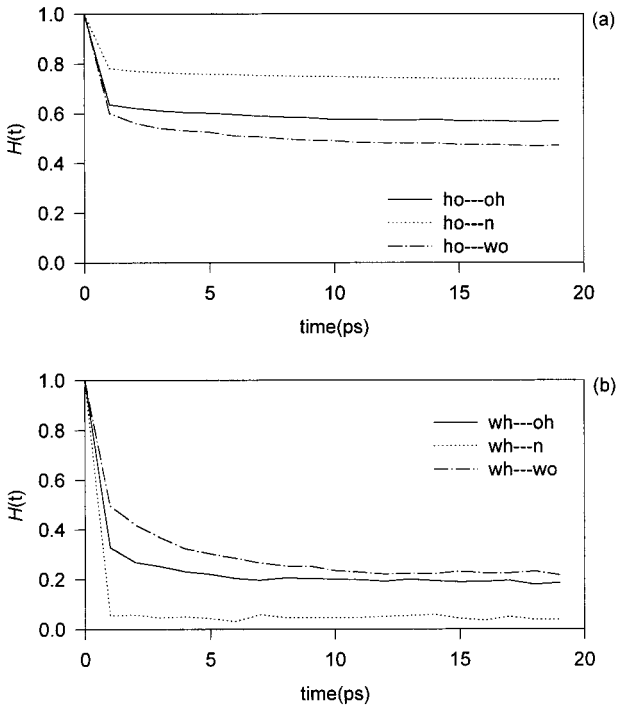

Figure 12. Hydrogen bonding autocorrelation function $H(t)$ (a) of OH(PBO) and acceptor hydrogen bonds and (b) of OH-(water) and acceptor hydrogen bonds at 295 K.

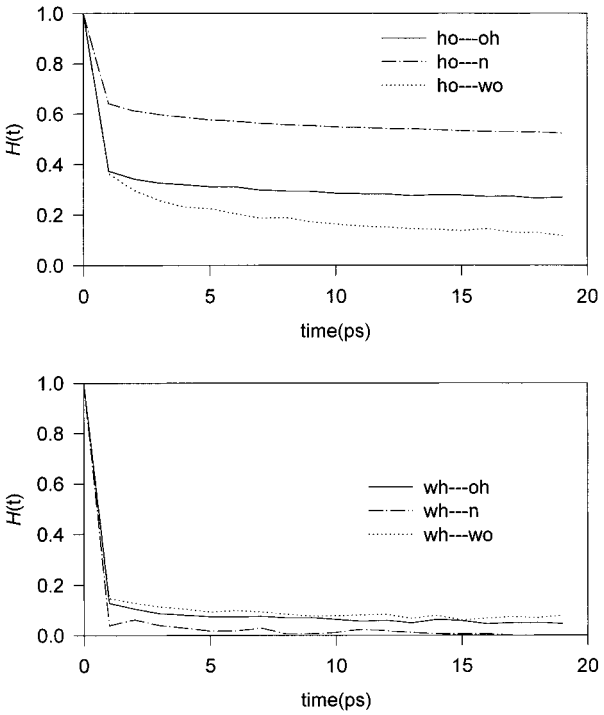

Figure 13. Hydrogen bonding autocorrelation function $H(t)$ (a) of OH (PBO) and acceptor hydrogen bonds and (b) of OH (water) and acceptor hydrogen bonds at 450 K.

temperature because of the almost frozen polymer matrix. The surroundings around H_2O are very different from those of O_2, which can be seen in the radial distribution function.

The jump event of H_2O in the PBO matrix requires less than 1 ps at both temperatures. In this time interval, the averaged absolute displacement of each atom type was obtained as a function of the distance from the diffusant. At 295 K, only methyl side groups

attached to the phenyl ring have higher mobility near the site of the jump event. In contrast, all types of atoms near the jump event have higher displacements than those away from the jump event at 450 K. About 65% of hydroxy groups in PBO at 295 K and 57% of them at 450 K were found to have hydrogen bonds with the acceptors of nitrogen and oxygen atoms in PBO and oxygen atom in water. About 60% of the acceptors were provided from the nitrogen atom at both temperature. Almost 38% of the hydroxy groups in H_2O participated in hydrogen bonding with the acceptors of oxygen and nitrogen atom in PBO and oxygen in water. More than 50% of the acceptors were provided by the oxygen in PBO and about 35% of acceptors by the oxygen atom in H_2O. Nitrogen atoms hardly formed hydrogen bonds with H_2O.

The lifetime of hydrogen bonds between donors and acceptors provided by PBO is longer than the lifetime of hydrogen bonds with H_2O. Generally, the lifetime is proportional to the averaged number of hydrogen bonds calculated, on the basis of the hydrogen bond correlation function. The lifetime of hydrogen bonds of H_2O is found to be on the time scale of several picoseconds. This time scale is much shorter than the residence time of a diffusant in a cavity, and therefore, the hydrogen bonding does not retard the diffusion of the penetrants. In this sense, the predicted diffusion coefficient of H_2O in a PBO matrix is strikingly close to that of O_2, although H_2O forms hydrogen bonds with the PBO matrix but O_2 does not.

Acknowledgment. This research was supported by the Federal Aviation Administration.

References and Notes

(1) *Diffusion in Polymers*; Crank, J., Park, G. S., Ed.; Academic: London, 1968.
(2) *Polymer Permeability*; Comyn, J., Ed.; Elsevier: London, 1985.
(3) Vieth, W. R. *Diffusion in and through Polymers*; Hanser: Munich, 1991.
(4) Gusev, A. A.; Müller-Plathe, F.; van Gunsteren, W. F.; Suter, U. W. *Adv. Polym. Sci.* **1994**, *116*, 207.
(5) Gusev, A. A.; Suter, U. W. *J. Chem. Phys.* **1993**, *99*, 2228.
(6) Sonnenburgh, J.; Gao, J.; Weiner, J. H. *Macromolecules* **1990**, *23*, 4653.
(7) Takeuchi, H. *J. Chem. Phys.* **1990**, *93*, 2062.
(8) Takeuchi, H.; Roe, R. J.; Mark, J. E. *J. Chem. Phys.* **1990**, *93*, 9042.
(9) Boyd, R. H.; Pant, P. V. K. *Macromolecules* **1991**, *24*, 6325.
(10) Pant, P. V. K.; Boyd, R. H. *Macromolecules* **1992**, *25*, 494.
(11) Trohalaki, S.; Kloczkowski, A.; Mark, J. E.; Roe, R. J.; Rigby, D. *Comput. Polym. Sci.* **1992**, *2*, 147.
(12) Müller-Plathe, F. *J. Chem. Phys.* **1992**, *96*, 3200.
(13) Sok, R.; Berendsen, H.; van Gunsteren, W. *J. Chem. Phys.* **1992**, *96*, 4699.
(14) Müller-Plathe, F.; Rogers, S. C.; van Gunsteren, W. F. *Macromolecules* **1992**, *25*, 6722.
(15) Müller-Plathe, F.; Rogers, S. C.; van Gunsteren, W. F. *Chem. Phys. Lett.* **1992**, *199*, 237.
(16) Pant, P. V. K.; Boyd, R. H. *Macromolecules* **1993**, *26*, 679.
(17) Gusev, A. A.; Arizzi, S.; Suter, U. W.; Moll, D. *J. Chem. Phys.* **1993**, *99*, 2221.
(18) Tamai, Y.; Tanaka, H.; Nakanishi, K. *Macromolecules* **1994**, *27*, 4498.
(19) Han, J.; Boyd, R. H. *Macromolecules* **1994**, *27*, 5365.
(20) Zhang, R.; Mattice, W. L. *J. Membr. Sci.* **1995**, *108*, 15.
(21) Gusev, A. A.; Suter, U. W.; Moll, D. J. *Macromolecules* **1995**, *28*, 2582.
(22) Han, J.; Boyd, R. H. *Polymer* **1996**, *37*, 1797.
(23) Fujita, H. *Fortschr. Hochpolym.-Forsch.* **1961**, *3*, 1.
(24) Barrer, R. M.; Chio, H. T. *J. Polym. Sci.* **1965**, *C10*, 111.
(25) Tikhomirov, B. P.; Hopfenberg, H. B.; Stannett, V.; Williams, J. L. *Makromol. Chem.* **1968**, *118*, 177.
(26) Cicerone, M. T.; Blackburn, F. R.; Ediger, M. D. *Macromolecules* **1995**, *28*, 8224.
(27) Sun, H.; Mumby, S. J.; Maple, J. R.; Hagler, A. T. *J. Am. Chem. Soc.* **1994**, *116*, 1994.
(28) Sun, H. *J. Comput. Chem.* **1994**, *15*, 752.
(29) Sun, H. *Macromolecules* **1995**, *28*, 701.
(30) Kim, W.-K.; Mattice, W. L. *Comput. Theor. Polym. Sci.*, in press.
(31) Fritz, L.; Hofmann, D. *Polymer* **1997**, *5*, 1035.
(32) Ishida, H.; Allen, J. D. *J. Polym. Sci., Part B: Polym. Phys.* **1996**, *34*, 1019.
(33) Ishida, H.; Krus, C. M. *Macromolecules* **1998**, *31*, 2409.

MA9806662